THE FREQUENCY RESPONSE OF SONIC ANEMOMETERS

C. WAMSER
Alfred-Wegener-Institute for Polar and Marine Research, Bremerhaven, Germany
G. PETERS
Meteorological Institute, University of Hamburg, Hamburg, Germany
V. N. LYKOSSOV
Institute for Numerical Mathematics, Russian Academy of Sciences, Moscow, Russia

(Received in final form 28 February, 1997)

Abstract. The frequency response of different types of sonic anemometers due to spatial averaging of turbulent fluctuations along the sonic path is investigated by applying modeling procedures and by sonic measurements. The data were obtained simultaneously at up to 4 heights over extreme smooth and homogeneous terrain during stationary situations, varying from slightly stable to unstable. It is shown that corrections for the variance of the vertical wind component are needed for measurements close to the ground. A correction procedure, based on a response function for the vertical wind and on parameters derived from power spectra, is applied to the measurements. At a height of about one metre, the variance of the vertical wind component is typically underestimated by about 10%. The error decreases with increasing height. It is also shown that in the height range down to one metre other turbulence quantities, as for example the variances of the horizontal wind components and the turbulent fluxes of momentum and sensible heat, are not markedly affected by the sonic spatial response. Experimental data support these findings.

Key words: Sonic anemometers, Frequency response, Spatial averaging, Turbulent fluctuations

1. Introduction

During recent times the sonic anemometer technique has become a basic research tool for the determination of the turbulent fluxes of momentum and sensible heat in the atmospheric boundary layer. Compared to other wind measuring systems, sonic sensors have several advantages, such as high response, no overshooting, no inertia. Complicated technical handling of earlier times has been changed to a modest treatment of the instruments and manufacturer's prices are nowadays affordable by research and commercial users. Errors of sonic techniques due to disturbances of the flow by the ultrasonic transducers (e.g., Horst, 1973; Grant and Watkins, 1989; Wyngaard and Zhang, 1985) have been significantly reduced by appropriate mechanical design of the sensor array, e.g., by hiding the transducers in a streamlined ring and by avoiding flow directions parallel to the transmitter/receiver units. Spurious readings of sonic measurements by accumulation of snow and rime on the transducers have been reported by King (1990). Such effects can easily be avoided by adequate heating of the sensors. The impact of particles, such as ice crystals and rain drops on the transducers, may reduce the accuracy of turbulence measurements with sonic instruments. But since these influences cause distinct spikes in the data series, they can be corrected with the aid of special algorithms.

Boundary-Layer Meteorology **84:** 231–246, 1997.

One main restriction of the sonic technique, however, especially at lower measurement heights, is due to the fact that the response to small-scale turbulent fluctuations is limited, since the measured transit times of the acoustic pulses, travelling along the paths between the acoustic transmitters and receivers, represent line-averaged velocities. This leads to low-pass filtering, so that the high frequency turbulence is suppressed in the record, as discussed e.g., by Horst (1973), Kaimal et al. (1968) and Kristensen and Fitzjerrald (1984). Kaimal (1986) recommended use of sonics only above the minimum measuring height $z = 8\pi l$, with l the transmitter-receiver path length.

We will focus mainly on the influence of spatial averaging on the second moments of the turbulence. In Section 2 the theoretical background, based on the use of a spectrum model, is presented. Section 3 gives an overview of results from measurements, where sonic systems were used simultaneously at different heights close to the surface. For this purpose data from flat and homogeneous upwind surfaces under rather stationary atmospheric conditions are utilized, in order to avoid contamination of the data by arbitrary local surface structures. We find that the usable height range can be significantly extended below the above mentioned limit, at least under near neutral and unstable conditions. For the most affected quantity, the vertical wind fluctuations, a correction scheme is suggested. In the Appendix the analytical evaluation of the variance error equation is presented.

2. Theoretical Background

According to Kaimal et al. (1968), the variance of the vertical wind component is expressed by the integral over the one-dimensional spectral density

$$u_{33} = \int_0^\infty S_{33}(k_1)dk_1 \tag{1}$$

with

$$S_{33}(k_1) = \int_{-\infty}^{\infty}\int_{-\infty}^{\infty} \Phi_{33}(\mathbf{k})\, \mathrm{d}k_2\, \mathrm{d}k_3. \tag{2}$$

Here, $\Phi_{33}(\mathbf{k})$ is a component of the spectral density tensor, k_1 is the horizontal wave number parallel to the mean flow, which can be derived from measurements at a fixed point using the Taylor hypothesis, k_2 and k_3 are the cross-stream and vertical wave numbers respectively. As a consequence of spatial filtering of the measured data one actually obtains averaged values, expressed by

$$\tilde{u}_{33} = \int_0^\infty \tilde{S}_{33}(k_1)dk_1. \tag{3}$$

Kaimal et al. (1968) derived a transfer function $T_{33}(k_1)$

$$\tilde{S}_{33}(k_1) = T_{33}(k_1)S_{33}(k_1), \tag{4}$$

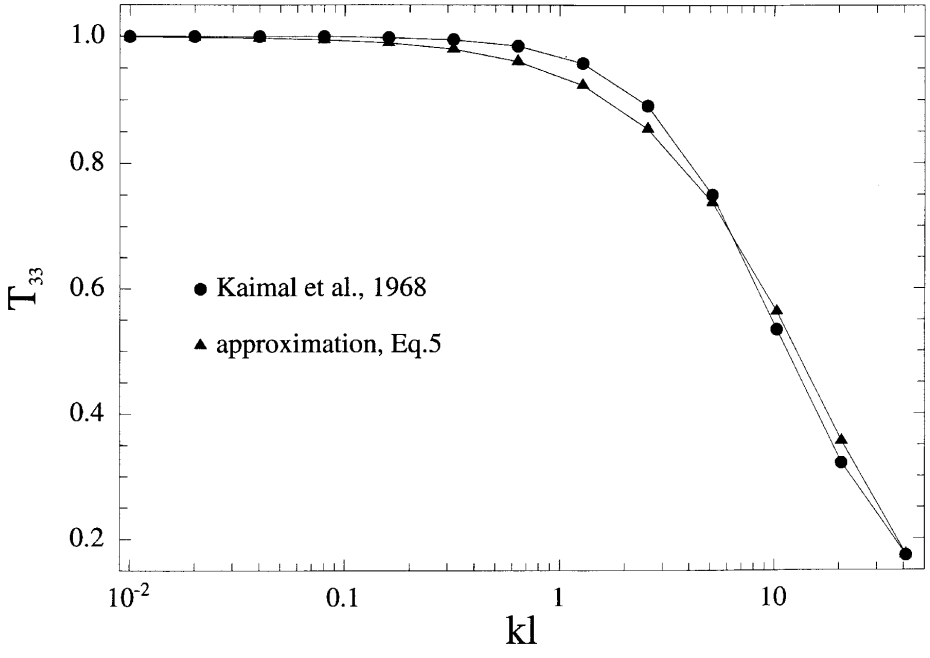

Figure 1. Transfer function T_{33} as a function of wave number k and sonic path length l. The approximation of the function (see text) is indicated by the triangles.

which relates $\tilde{S}_{33}(k_1)$ to the real value $S_{33}(k_1)$ for a vertically oriented measuring path. Here, the assumption of isotropic turbulence is made and a spatial averaging effect is assumed to be significant in the inertial subrange of the velocity variance spectrum. The sonic data discussed in this paper are not derived from a vertically oriented path, but rather by combining the components measured on 3 paths with 45° inclination and an azimuth angle of 120°.

Although no transfer function has been published for this configuration, we will apply Equation (4) at least for small corrections. In order to obtain simple algebraic expressions for the correction of $\tilde{u}_{33}$, we approximate the transfer function by

$$T_{33} = \frac{1}{(1+\beta lk)^{\nu}} \tag{5}$$

where $k \equiv k_1$, l is the sonic path length, β and ν are numerical constants. Figure 1 shows the original transfer function T_{33} for a vertical sonic cross-probe and the above suggested approximation, according to Equation (5), with $\beta = 0.0272$ and $\nu = 7/3$.

The variance spectrum of the vertical wind component is approximated by the function

$$S_{33}(k) = \frac{Ak^s}{(1+Bk)^{5/3+s}}, \tag{6}$$

where s is the slope of the spectrum at the lower frequency range, A and B are constants that depend on atmospheric conditions. This form of the spectrum is a particular case of a more general expression, presented by Olesen et al. (1984). Such spectra are characterized by a high-frequency slope of $-5/3$ on a log-log plot, resulting from Kolmogoroff's law for the inertial subrange. Values of the low-frequency slope s, reported in the literature, vary significantly. Kaimal et al. (1972) and Olesen et al. (1984) found a value close to zero. From data of Garratt (1972) a slope of about $-2/3$ can be derived. Kader and Yaglom (1991) found s to be close to -1. By insertion of the transfer function T_{33} and the variance spectrum S_{33} into Equation (3) we can express the measured variance by

$$\tilde{u}_{33} = A \int_0^\infty \frac{k^s\, dk}{(1 + Bk)^{5/3+s}(1 + \beta lk)^\nu}. \tag{7}$$

This variance has to be compared with the true variance

$$u_{33} = A \int_0^\infty \frac{k^s\, dk}{(1 + Bk)^{5/3+s}}. \tag{8}$$

As a result, the relative error of the measured value can be derived

$$\Delta = \frac{\tilde{u_{33}} - u_{33}}{u_{33}}. \tag{9}$$

To estimate Δ, the following form of the power spectrum is used (e.g., Olesen et al., 1984; Panofsky and Dutton, 1984)

$$\frac{nS_{33}(n)}{u_*^2} = \frac{A_0(f/\phi_m)^{s+1}}{(1 + B_0 f/\phi_m)^{s+5/3}} \left(\frac{\phi_\epsilon}{\phi_m}\right)^{2/3}, \tag{10}$$

where n is the frequency, f is the reduced frequency, $f = nz/U$, U is the mean wind speed and u_* is the friction velocity. Based on criteria formulated by Olesen et al. (1984), we choose the constants A_0 and B_0 as depending on the position f_{mn} of the spectral maximum, observed for neutral conditions, and on the slope s. From this, it follows that

$$A_0 = \frac{4}{3} C_0 B_0^{s+5/3}, \quad B_0 = \frac{3(s+1)}{2f_{mn}}, \quad C_0 = \frac{\alpha_1}{(2\pi\kappa)^{2/3}}, \tag{11}$$

where $\kappa = 0.4$ is the von Kármán's constant, and α_1 is a universal constant; from various experiments a value of 0.5 is used (Kaimal et al., 1972). Values of f_{mn}, reported in the literature, vary from 0.25 to 0.55. Based upon data from the Kansas and Minnesota experiments, Olesen et al. (1984) used $f_{mn} = 0.35$ and $s = 0$, by which followed that $A_0 = 4.6$ and $B_0 = 4.3$. In the following section we will use

varying parameters s and f_{mn}, which we derive from the observed power spectra for various experiments.

The function ϕ_m in Equation (10) is the dimensionless vertical wind shear, which depends on the atmospheric stability

$$\phi_m(z/L) = \begin{cases} 0.37 & \text{for } z/L \leq -3.6 \\ (1 - 15z/L)^{-1/4} & \text{for } -3.6 < z/L \leq 0, \\ 1 + 4.7z/L & \text{for } z/L > 0 \end{cases} \tag{12}$$

where z is the measuring height and L is the Obukhov length, determined with the friction velocity u_*, temperature T and the covariance $\langle u_3 T \rangle$ measured with the sonic systems

$$L = -\frac{T u_*^3}{\kappa g \langle u_3 T \rangle}, \tag{13}$$

where g is the acceleration of gravity.

For the dimensionless dissipation rate ϕ_ϵ an expression from Panofsky and Dutton (1984) is used

$$\phi_\epsilon = \phi_m - \frac{z}{L}. \tag{14}$$

Since $k = 2\pi n/U = 2\pi f/z$, Equation (10) is related to (6) with

$$A = A_0 u_*^2 \left(\frac{z}{2\pi\phi_m}\right)^{s+1} \left(\frac{\phi_\epsilon}{\phi_m}\right)^{2/3}, \quad B = \frac{B_0 z}{2\pi\phi_m} = \frac{3(s+1)z}{4\pi f_m}, \tag{15}$$

where $f_m = f_{mn}\phi_m$. From (9) the following correction function for the measured variance of the vertical wind component can be derived

$$u_{33-corr.} = \frac{u_{33-meas.}}{1 + \Delta}. \tag{16}$$

The relative error Δ of the measured variance can be derived by numerical integration of the measured power spectrum and the transfer function T_{33}. Another method to determine Δ, and to investigate its dependence on the environmental and spectral parameters, is to find an analytical solution of the integrals (7) and (8). The integration is not simple and straightforward and requires the use of gamma and Gauss functions. The procedure, including a general presentation of the dependences, is given in Appendix A. For the case where the quotient of the measuring height z and the sonic path length l is much greater than unity the equation simplifies to

$$\Delta = -C_1 H_1(s, f_m) \left(\frac{z}{l}\right)^{-2/3}. \tag{17}$$

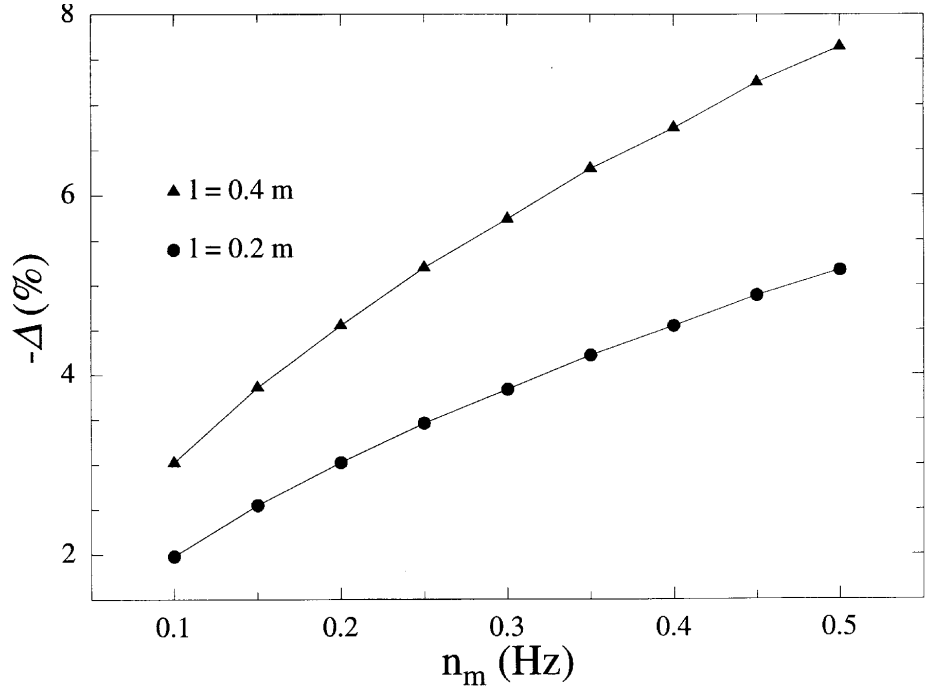

Figure 2. The variance error Δ as a function of two sonic path lengths and of the peak frequency n_m.

where the constant C_1 = 1.586 reflects the effect of spatial filtering and H_1 determines the dependence of the variance error on the spectrum parameters s and n_m. In Figure 2 an example is presented that shows the dependence of Δ on two typical sonic path lengths (0.2 and 0.4 m) and on the peak frequency n_m of the spectrum of the vertical wind component. Here, a measuring height of 5 m, near neutral stability, a moderate wind velocity of 5 m s^{-1}, a friction velocity of 0.2 m s^{-1} and a mean low frequency slope of the vertical wind spectrum of -0.66 are assumed. The frequency range between 0.1 and 0.5 Hz is, corresponding to our sonic measurements, typical for n_m in this height range and stabilities from unstable to stable stratifications. Here, Δ varies by a factor of about 2.4.

Transfer functions for the variances of the horizontal wind components (Kaimal et al., 1968) can also be approximated by a similar function (5) with $\nu = 7/3$ and β equal to 0.0524 for u_{11} and 0.0438 for u_{22}. Spectral models for these quantities are given by Kaimal et al. (1972) and have a similar form as our Equation (10). From this, it follows that our analysis, if needed, could easily be extended to the horizontal wind components. Transfer functions for the turbulent fluxes, however, are not published to our knowledge. On the other hand, it is known that contributions to the covariances in the high frequency range ($>$ 2 Hz) are negligible and corresponding peak frequencies are, in comparison to the vertical wind component, shifted to the

lower end of the spectrum. This means that the sonic filter effect should be very small, even for measurements close to the ground.

3. Sonic Measurements

Four experiments with high-resolution sonic measurements were used to apply the approximations, presented in the previous section. The measuring conditions were characterized by smooth and homogeneous surfaces and stationarity of the meteorological conditions. The roughness lengths of the surfaces at the different sites, derived from our turbulence measurements, were small with values between 0.01 and 0.3 mm. The measurements, presented below, were selected with regard to homogeneity of the sites, stationarity of the conditions and to the range of stability from unstable to stable stratification. For three of the experiments, simultaneous high resolution turbulence measurements at at least two different heights were available. A short description of the experiments is given below.

ARCTIC: Four USAT-3 instruments (l = 0.4 m) were exposed at the heights of 4, 6, 8, 20 m at a meteorological mast on the bow crane of the German research vessel Polar Stern (PS). The measurements were conducted in the Fram Strait within a 2 km wide polynya, covered with a thin new ice layer of about 5 cm thickness. The stratification of the near-surface air was unstable. A description of the site and the measurements is given by Wamser and Lykossov (1996).

ANTARCTIC: A Kaijo Denki (DAT 300) sensor was installed on the vessel PS at 14.7 m above the sea-ice in the Atka Bight, close to the Antarctic shelf ice of the Weddell Sea. The sea ice cover was very smooth and snow drift from the coast was observed. The surface layer was stably stratified. Details of the measurements are presented by Lykossov and Wamser (1995).

NORTH SEA (measuring intervals I-IV): At the beach of the North Sea two instruments of the type USA-1 (l = 0.18 m) and USAT-3 (l = 0.4 m) were exposed at 1.7 and 3.0 m, respectively. The upwind fetch of about 300 m was very flat and homogeneous. Sand drift close to the surface was observed during two of the four measuring intervals. The vertical density distribution in the surface layer was continuously unstable. Measurements were taken for about one hour in each case.

WESER (measuring intervals I-IV): During a field study over the tidal flats of the river Weser four USAT-3 systems were applied in the height range 1.4 to 3.5 m, above the surface. No obstacles were present at the moist surface, even at large upstream distances. The static stability of the surface layer ranged from near neutral to slightly unstable. Some gross information on the observational conditions during the four field studies is listed in Table I.

Table I

Mean meteorological conditions: Monin–Obukhov stability parameter $1/L$, wind velocity U, measuring height z and path lengths l of sonic instruments, used in this paper

EXPERIMENT	$1/L$ (m^{-1})	U (m s^{-1})	z (m)	l (m)
ARCTIC	−0.0196	5.7	4, 6, 8, 20	0.4
ANTARCTIC	0.0022	15.9	14.7	0.2
NORTH SEA-I	−0.0462	6.4	1.7, 3.0	0.18, 0.4
NORTH SEA-II	−0.0202	6.9	1.7, 3.0	0.18, 0.4
NORTH SEA-III	−0.0185	7.4	1.7, 3.0	0.18, 0.4
NORTH-SEA IV	−0.0064	8.4	1.7, 3.0	0.18, 0.4
WESER-I	0.0021	4.5	1.4, 3.0	0.4
WESER-II	−0.0016	4.1	1.4, 3.0	0.4
WESER-III	−0.0152	3.8	1.4, 3.5	0.4
WESER-IV	−0.0265	3.2	1.4, 3.5	0.4

Spectral parameters, such as the peak frequency and the spectral slope in the low-frequency range, are needed to apply the correction procedure, given in Section 2 and in the Appendix. Smoothed variance spectra of the kind shown in Figure 3 (experiment ARCTIC) are determined through Fast Fourier Transformation of the detrended series. The spectral range, with the Nyquist frequency of 8.5 Hz at the high frequency limit, depends on the number of lags. In this case the spectra were determined over 42 intervals of 2048 data points each. This procedure leads to a lowest frequency of 0.008 Hz and results in high significance of the spectra. The positions of the spectral maxima n_m are indicated by the arrows and show the expected shift to lower frequencies with height. The low frequency slopes of the spectra are similar in the four height ranges, having a mean value of -0.75.

A comparison between measured and approximated variance spectra is shown in Figure 4. The dots are the measured, and the circles the modelled, spectra on a log–log plot. The data are presented corresponding to Equation (10), normalized by the frequency n and by $(\phi_\epsilon/\phi_m)^{2/3}$. There is excellent agreement. In the inertial subrange the spectra are close to the expected $-5/3$ slope. Small deviations from this law, especially pronounced close to the ground, could possibly be due to two opposite effects viz, the attenuation of the contributions in the high frequency range by path-length-averaging and the well-known enhancement by aliasing. The low-frequency range is characterized by a nearly constant $-3/4$ slope.

Table II shows the results of the four experiments, consisting of 10 runs. Here are given the quantities, which are needed to calculate the function Δ and to correct the observed u_{33}-variances. The data comprise the height range 1.4 to 20 m, wind speeds, and stabilities from unstable to stable. Our data, presented here from very different sites, show remarkably small scatter of the slope s, with a mean value of

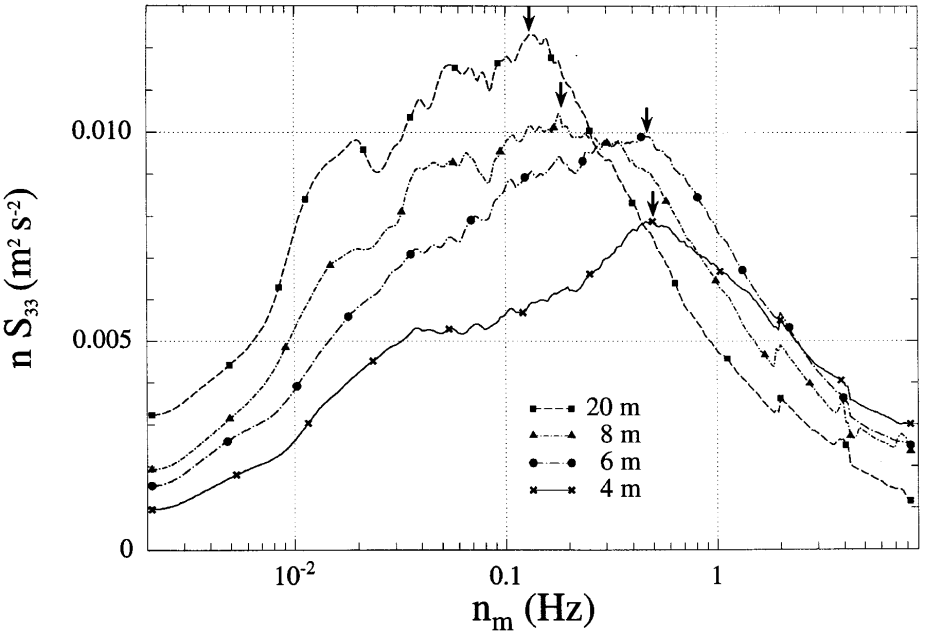

Figure 3. Variance spectra of the vertical wind component, measured at 4 heights above the sea ice surface (experiment ARCTIC).

-0.63 ± 0.11. It is obvious from the Table that the error Δ varies with measuring height and sonic path length. The greatest differences, of more than 10%, arise during the experiment WESER, where sonic systems with l = 0.4 m were used close to the ground.

Figure 5 summarizes the results of the variance error Δ for the vertical wind component as function of the ratio of the geometric parameters z and l. It is seen, that the slope of the regression line on the log-log plot is close to $-2/3$. This agrees with the analytical prediction, presented in Appendix A. The scatter of the data points is due to the influence of stability and other environmental characteristics. Most of the commercially available sonic systems use path lengths between 0.1 and 0.4 m. Our analysis shows, that the output data of these instruments need to be corrected, when measurements are taken close to the earth's surface.

From theoretical considerations and recent observations there seems to be no critical height limitation for sonic measurements, from which the variances u_{11}, u_{22} and turbulent fluxes are to be derived (Kristensen and Fitzjarrald, 1984). This conclusion goes along with observational facts that the peaks of the u- and v-spectra lie at significantly lower wave numbers k than those of the vertical wind component. An example of variance spectra of the horizontal wind components and cospectra of momentum and sensible heat fluxes, measured at 3, 6 and 8 m above the sea-ice surface during the experiment ARCTIC, is portrayed in Figure 6.

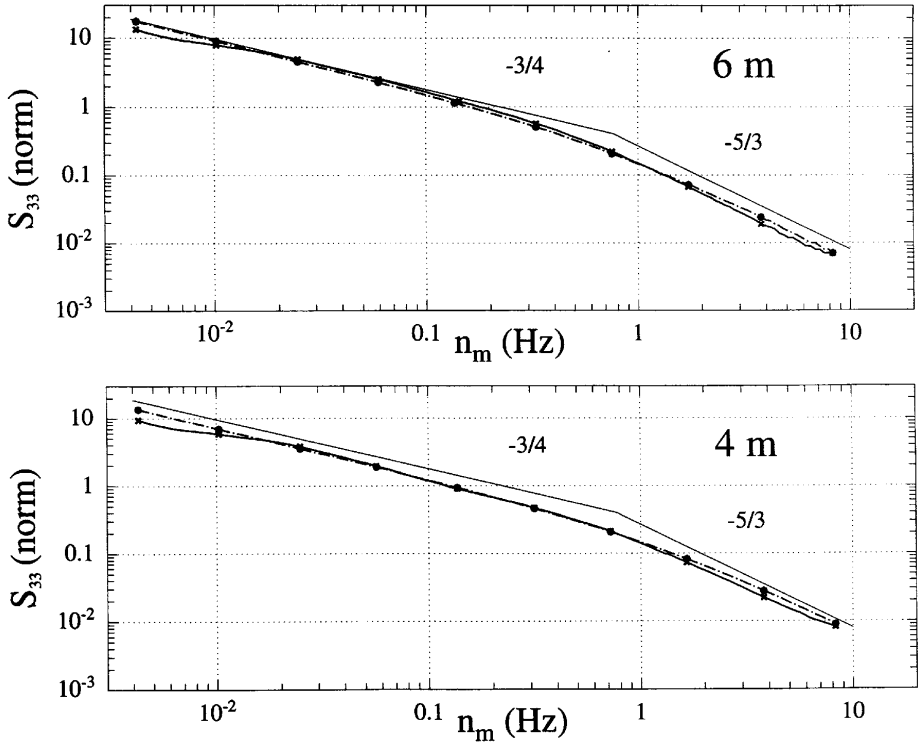

Figure 4. Measured (crosses) and approximated (dots) variance spectra of the vertical wind component (experiment ARCTIC).

In comparison to the vertical wind compoment there is a clear shift of the spectral maximum to lower frequencies close to about 0.02 Hz in this case. Kaimal et al. (1972) found for near neutral stability the following relationship for the normalized peak frequencies f_m

$$(f_m)_w \simeq 5(f_m)_u \simeq 2(f_m)_v.$$

Even in stable situations the total variances u_{11} and u_{22} have their major contributions in the low frequency range of the spectrum (Bush, 1973). Similar behaviour is found for the cospectra of $\langle u_1 u_3 \rangle$ and $\langle u_2 u_3 \rangle$. At high frequencies the turbulence is more or less isotropic, so that these wave numbers do not contribute to the turbulent transport of momentum. Therefore it seems plausible to expect not such a clear height limitation as for the vertical wind component.

4. Concluding Remarks

The effect of path line averaging on the measurement of the second moments of turbulence in the surface layer has been investigated. For the most affected

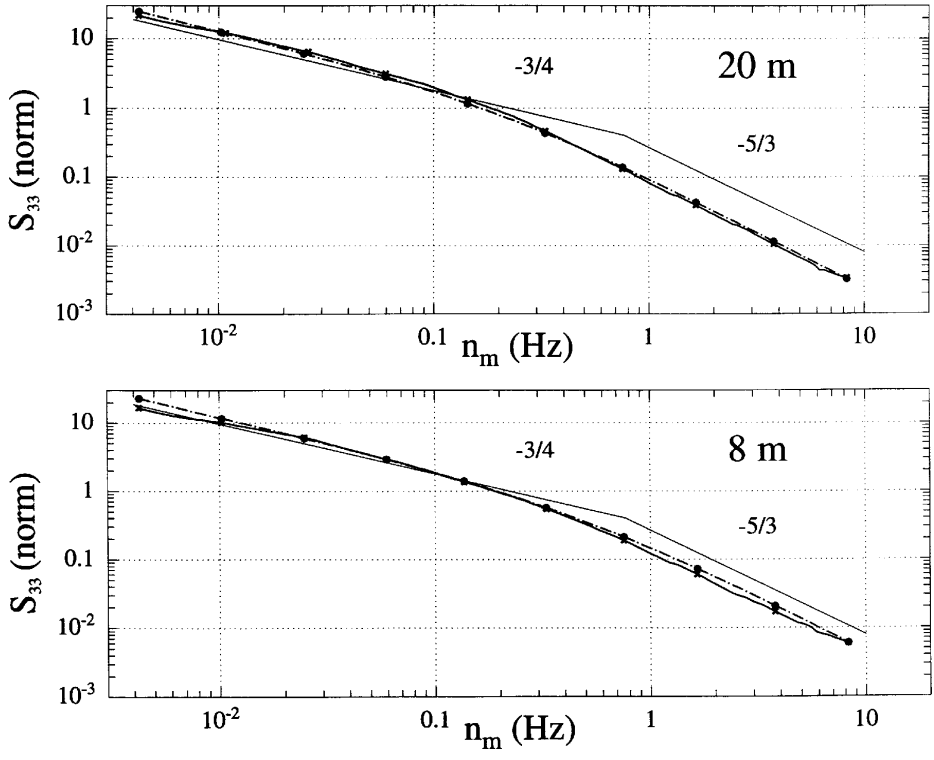

Figure 4.

variable, the variance of the vertical wind component u_{33}, a maximum attenuation of $\Delta = 15$ % has been found very close to the surface, and a stability dependent correction has been suggested. This attenuation occured at the lowest measuring height of $z \approx 4l$, where l is the transmitter-receiver path length. For other second moments containing horizontal wind components or for the vertical sensible heat and momentum fluxes the attenuation is expected to be much smaller, so that no correction is required. From this we conclude that Kaimal's recommendation of a minimum measuring height $z = 8\pi l$ can be significantly relaxed, at least for unstable to slightly stable conditions, as prevailed in the field tests reported here.

Acknowledgment

The authors wish to express their thanks to Professor Ernst Augstein and Dr. Christoph Kottmeier, who made constructive comments on an early draft of this paper. We also thank the editor and the two anonymous reviewers for their helpful comments. We are grateful to all of our colleagues who helped in the field and the data analysis. V. Lykossov thanks the Russian Fund for Fundamental Investigations

Table II

Environmental and spectral quantities for 4 experiments. Names of experiments are abbreviated. The last two columns give the measured and corrected variances of the vertical wind component

EXP.	l m	z m	z/L	U m s^{-1}	u_* m s^{-1}	n_m s^{-1}	s	Δ %	u_{33m} m^2 s^{-2}	u_{33c} m^2 s^{-2}
ARC.	0.40	4.0	−0.078	5.64	0.212	0.62	−0.79	−7.1	0.0396	0.0426
	0.40	6.0	−0.128	5.83	0.215	0.34	−0.77	−5.1	0.0511	0.0539
	0.40	8.0	−0.163	5.95	0.214	0.20	−0.74	−3.9	0.0542	0.0564
	0.40	20.0	−0.342	6.38	0.212	0.09	−0.71	−2.4	0.0610	0.0625
ANT.	0.20	14.7	0.032	15.88	0.488	0.20	−0.59	−1.6	0.3758	0.3817
N.S.-I	0.18	1.7	−0.102	6.09	0.184	0.98	−0.93	−3.8	0.0698	0.0726
	0.40	3.0	−0.097	6.68	0.234	0.50	−0.63	−6.7	0.0722	0.0774
N.S.-II	0.18	1.7	−0.033	6.54	0.266	0.90	−0.57	−6.2	0.0841	0.0896
	0.40	3.0	−0.063	7.19	0.260	0.55	−0.60	−6.9	0.0874	0.0938
N.S.-III	0.18	1.7	−0.033	7.04	0.263	1.20	−0.55	−7.1	0.0904	0.0973
	0.40	3.0	−0.052	7.74	0.280	0.62	−0.55	−7.2	0.0956	0.1030
N.S.-IV	0.18	1.7	−0.011	7.91	0.311	1.30	−0.55	−6.9	0.1069	0.1148
	0.40	3.0	−0.020	8.81	0.310	0.80	−0.60	−7.6	0.1110	0.1201
W.-I	0.40	1.4	−0.003	4.34	0.171	0.95	−0.70	−11.3	0.0208	0.0234
	0.40	3.0	−0.007	4.71	0.147	0.60	−0.43	−9.8	0.0213	0.0236
W.-II	0.40	1.4	−0.003	3.92	0.141	1.30	−0.58	−15.2	0.0169	0.0199
	0.40	3.0	−0.004	4.25	0.155	0.70	−0.55	−10.7	0.0243	0.0272
W.-III	0.40	1.4	−0.022	3.60	0.119	0.95	−0.55	−14.1	0.0135	0.0157
	0.40	3.5	0.050	3.92	0.127	0.55	−0.60	−9.7	0.0187	0.0207
W. -IV	0.40	1.4	−0.035	3.05	0.121	0.90	−0.63	−13.9	0.0125	0.0145
	0.40	3.5	−0.098	3.26	0.120	0.45	−0.65	−9.2	0.0134	0.0148

for financial support (Grant 95-05-14172). This paper is the contribution number 1024 of the Alfred Wegener Institute for Polar and Marine Research.

Appendix A. Analytical Evaluation of the Relative Error Δ

Corresponding to Equation (7), the measured variance $\tilde{u}_{33}$ is expressed by

$$\tilde{u}_{33} = A \int_0^\infty \frac{k^s dk}{(1+Bk)^{5/3+s}(1+\beta lk)^\nu}, \tag{18}$$

from which follows, for $s > -1$,

$$\tilde{u}_{33} = \frac{A}{B^{s+1}} \mathbf{B}(\nu + 2/3, s+1)\, {}_2F_1(\nu, s+1; s+\nu+5/3; 1-\beta l/B). \tag{19}$$

Here, $\mathbf{B}(x,y) = \Gamma(x)\Gamma(y)/\Gamma(x+y)$ is the beta function, $\Gamma(x)$ is the gamma function, and ${}_2F_1(a,b;c;x)$ is the Gauss hypergeometric function. In order to

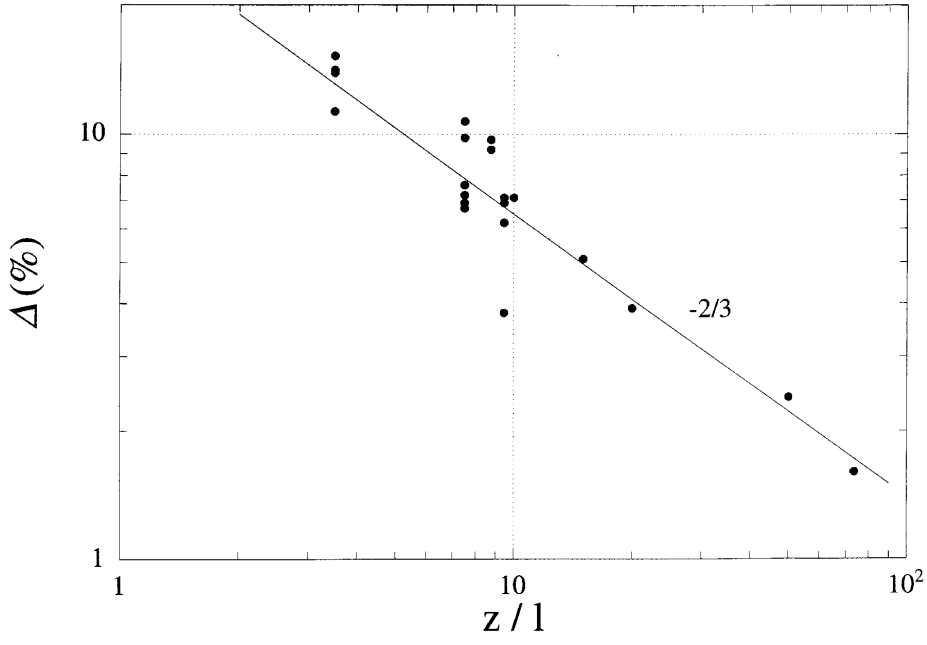

Figure 5. The variance error Δ as a function of z/l.

derive a practical form of $\tilde{u}_{33}$, we use the following identity (e.g., Gradshteyn and Ryzhik, 1980)

$$
{}_2F_1(a,b;c;x) = \Gamma(c)[\frac{\Gamma(c-a-b)}{\Gamma(c-a)\Gamma(c-b)}{}_2F_1(a,b;a+b-c+1;1-x)
$$

$$
+(1-x)^{c-a-b}\frac{\Gamma(a+b-c)}{\Gamma(a)\Gamma(b)}{}_2F_1(c-a,c-b;c-a-b+1;1-x)]. \qquad (20)
$$

The function ${}_2F_1(a,b;c;x)$ can be represented by a hypergeometric series

$$
{}_2F_1(a,b;c;x) = 1 + \frac{\Gamma(c)}{\Gamma(a)\Gamma(b)}\sum_{n=1}^{\infty}\frac{\Gamma(a+n)\Gamma(b+n)}{\Gamma(c+n)n!}x^n, \qquad (21)
$$

which terminates when a or b are equal to a negative integer or to zero. Otherwise, it absolutely converges at $|x| \leq 1$ if $c \neq -m$ (m =0, 1, 2, . . .).

For $\beta l/B << 1$, only the first two terms of the corresponding hypergeometric series need to be used. It is shown by our sonic measurements that this assumption generally holds. By applying (20), we then obtain from (19)

$$
\tilde{u}_{33} = \mathbf{B}(2/3, s+1)\left[1 + 3\nu(s+1)\frac{\beta l}{B}\right]\frac{A}{B^{s+1}}
$$

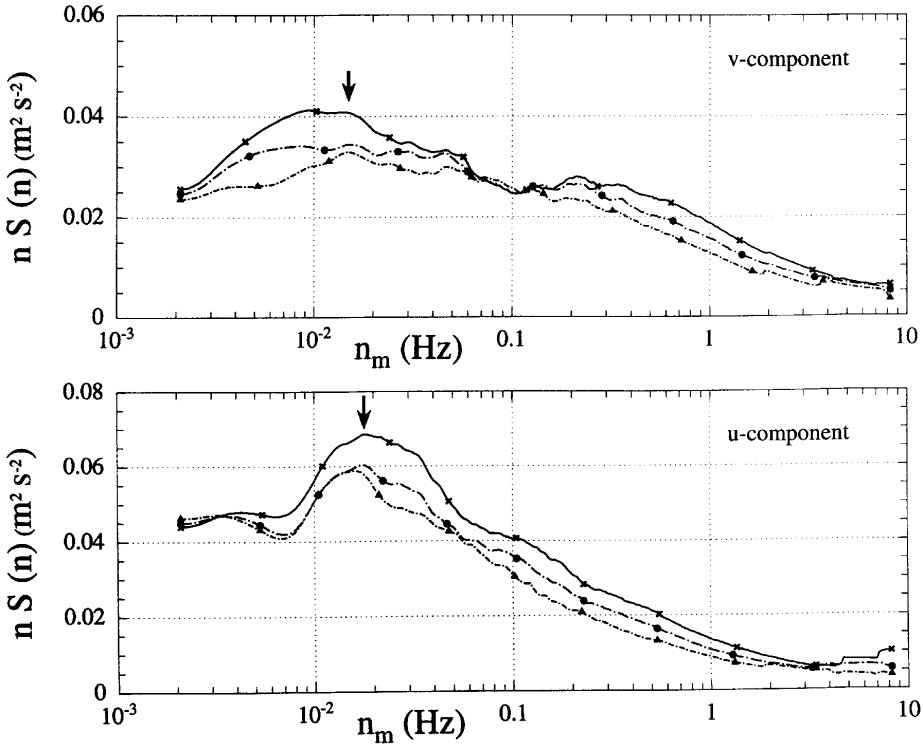

Figure 6. Examples of variance spectra of the horizontal wind components and cospectra of the sensible (upper) and momentum (lower) heat fluxes, measured at 4 m (crosses), 6 m (closed circles) and 8 m (triangles) above the sea-ice surface (experiment ARCTIC).

$$-\frac{\sqrt{3}\pi}{\mathbf{B}(2/3,\nu)}\left(\frac{\beta l}{B}\right)^{2/3}\left[1+\frac{3}{5}\left(s+\frac{5}{3}\right)\left(\nu+\frac{2}{3}\right)\frac{\beta l}{B}\right]\frac{A}{B^{s+1}}. \tag{22}$$

Assuming that in Equation (19) the filter parameters $\beta = \nu = 0$, one can also derive the following expression for the true variance u_{33}

$$u_{33} = \frac{A}{B^{s+1}}\mathbf{B}(2/3, s+1). \tag{23}$$

By comparing (22) and (23), we find the relative error of the measured variance

$$\Delta = \frac{\tilde{u}_{33} - u_{33}}{u_{33}} =$$

$$-\frac{\sqrt{3}\pi}{\mathbf{B}(2/3,s+1)\mathbf{B}(2/3,\nu)}\left[1+\frac{3}{5}\left(s+\frac{5}{3}\right)\left(\nu+\frac{2}{3}\right)\frac{\beta l}{B}\right]\left(\frac{\beta l}{B}\right)^{2/3}$$

$$+3\nu(s+1)\frac{\beta l}{B}. \tag{24}$$

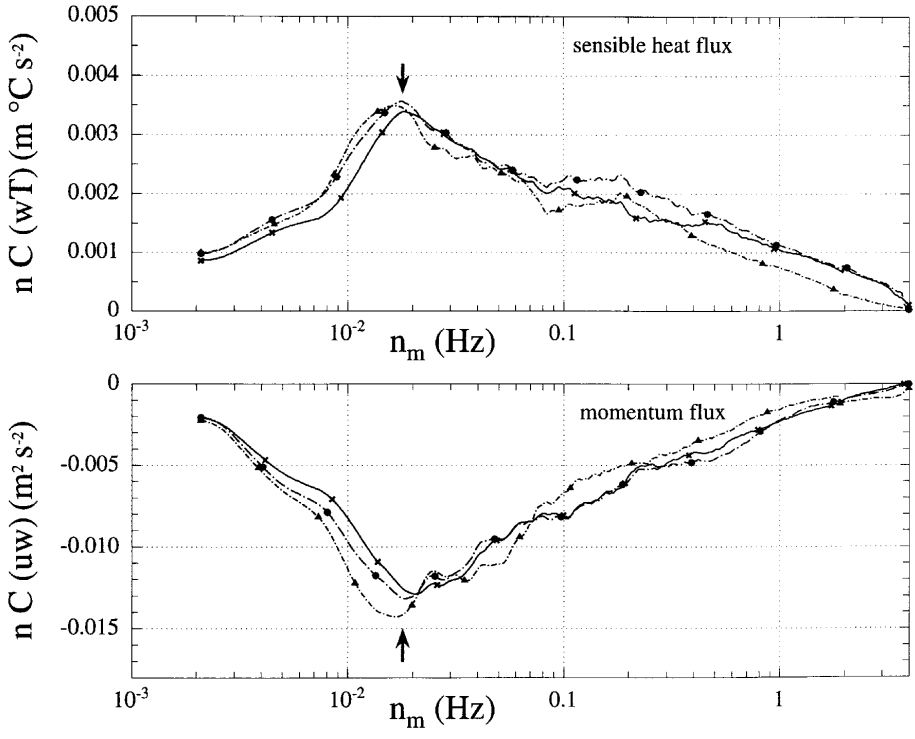

Figure 6.

It is obvious from Equation (24) that the relative error of the measured variance does not depend on the constant A, but is dependent on the value of the constant B which, corresponding to Equation (15), is proportional to z. It is also seen that the slope of the spectrum at the lower frequency range influences to a certain extent the magnitude of the variance error. By insertion of B from Equation (15) into (24), the relative error of the measured variance reads

$$\Delta = -C_1 H_1(s, f_m) \left(\frac{z}{l}\right)^{-2/3} \left[1 + C_2 H_2(s, f_m) \left(\frac{z}{l}\right)^{-1}\right] + C_3 f_m \left(\frac{z}{l}\right)^{-1}, \tag{25}$$

where

$$C_1 = \frac{\sqrt{3}\pi^{5/3}}{\mathbf{B}(2/3, \nu)} \left(\frac{4\beta}{3}\right)^{2/3}, \quad C_2 = \frac{4\pi\beta}{5}\left(\nu + \frac{2}{3}\right), \quad C_3 = 4\pi\beta\nu,$$

$$H_1(s, f_m) = \frac{1}{\mathbf{B}(2/3, s+1)} \left(\frac{f_m}{s+1}\right)^{2/3}, \quad H_2(s, f_m) = \frac{(s + 5/3) f_m}{s+1}. \tag{26}$$

Here, the constants C_1, C_2 and C_3 reflect the effect of spatial filtering. Since $\nu = 7/3$ and $\beta = 0.0272$, it follows that $C_1 = 1.586$, $C_2 = 0.205$ and $C_3 = 0.798$. The functions $H_1(s, f_m)$ and $H_2(s, f_m)$ show the dependence of the variance error Δ on the spectrum parameters. However, it is seen from Equation (25) that the major factor influencing the value of Δ is the ratio of the measuring height z to the sonic path length l. It is quite natural that the filtering effect is negligible when z is large or l is small. For $z/l >> 1$, Equation (25) can be simplified as follows

$$\Delta = -C_1 H_1(s, f_m) \left(\frac{z}{l}\right)^{-2/3}. \tag{27}$$

References

Bush, N. E.: 1973, 'The Surface Boundary Layer', *Boundary-Layer Meteorol.* **4**, 213–240.

Garratt, J. R.: 1972, 'Studies of Turbulence in the Surface Layer over Water (Lough Neagh). Part II. Production and Dissipation of Velocity and Temperature Fluctuations', *Quart. J. Roy. Meteorol. Soc.* **98**, 642–657.

Gradshteyn, I. S. and Ryzhik, I. M.: 1980, *Table of Integrals, Series, and Products*, Academic Press, New York, 1160 pp.

Grant, A. L. M. and Watkins, R. D.: 1989, 'Errors in Turbulence Measurements With Sonic Anemometer', *Boundary-Layer Meteorol.* **46**, 181–194.

Horst, T. W.: 1973, 'Spectral Transfer Functions for a Three-Component Sonic Anemometer', *J. Appl. Meteorol.* **12**, 1072–1075.

Kader, B. A. and Yaglom, A. M.: 1991, 'Spectra and Correlation Functions of Surface Layer Atmospheric Turbulence in Unstable Thermal Stratification', in O. Metais and M. Lesieur (eds.), *Turbulence and Coherent Structures*, Kluwer Academic Publishers, Dordrecht, pp. 387–412.

Kaimal, J. C., Wyngaard, J. C., and Haugen, D. A.: 1968, 'Deriving Power Spectra from a Three-Component SAonic Anemometer', *J. Appl. Meteorol.* **7**, 827–837.

Kaimal, J. C., Wyngaard, J. C., Izumi, Y., and Cote, O. R.: 1972, 'Spectral Characteristics of Surface Layer Turbulence', *Quart. J. Roy. Meteorol. Soc.* **98**, 563–589.

Kaimal, J. C.: 1986, 'Flux and Profile Measurements from Towers in the Boundary Layer', in H. Lenschow (ed.), *Probing the Atmospheric Boundary Layer*, AMS, Boston, pp. 9–28.

King, J. C.: 1990, 'Some Measurements of Turbulence over an Antarctic Ice Shelf', *Quart. J. Roy. Meteorol. Soc.* **116**, 379–400.

Kristensen, L. and Fitzjarrald, D. R.: 1984, 'The Effect of Line Averaging on Scalar Flux Measurements with a Sonic Anemometer near the Surface', *J. Atmos. Oceanic Tech.* **1**, 138–146.

Lykossov, V. N. and Wamser, C.: 1995, 'Turbulence Intermittency in the Atmospheric Surface Layer Over Snow-Covered Sites', *Boundary-Layer Meteorol.* **72**, 393–409.

Olesen, H. R., Larsen, S. E., and Hojstrup, J.: 1984, 'Modeling Velocity Spectra in the Lower Part of the Planetary Boundary layer', *Boundary-Layer Meteorol.* **29**, 285–312.

Panofsky, H. A. and Dutton, J. A.: 1984, *Atmospheric Turbulence. Models and Methods for Engineering Applications*, Wiley-Interscience Publ., New York, 397 pp.

Wamser, C. and Lykossov, V. N.: 1996, 'High Resolution Turbulence Measurements Above Arctic Sea Ice', in M. A. Kallistratova (ed.), *Proceedings of the 8th International Symposium on Acoustic Remote Sensing and Associated Techniques of the Atmosphere and Oceans.* Moscow, pp. 7.13–7.18.

Wyngaard, J. C. and Zhang, S.: 1985, 'Transducer, Shadow Effects on Turbulence Spectra Measured by Sonic Anemometers', *J. Atmos. Oceanic Tech.* **2**, 548–558.